

35. DATA REPORT: LATE MIOCENE TO PLEISTOCENE DIATOMS FROM THE BLAKE RIDGE, SITE 997¹

Akihiro Ikeda,² Hisatake Okada,² and Itaru Koizumi²

INTRODUCTION

Ocean Drilling Program Site 997 is located on the Blake Ridge, which underlies a periphery of the subtropical central gyre and is under the profound influence of the warm saline Gulf Stream as well as the Western Boundary Undercurrent (WBUC), which carried the clastic materials to the Blake Ridge as sediment drift (Fig. 1). The shipboard study of nannofossils and sedimentary particles revealed a downward increase in sedimentation rate and a higher concentration of diatoms in three stratigraphic intervals (Shipboard Scientific Party, 1996). Thus, the stratigraphic change in diatom accumulation rate is important to understand the paleoceanographic and depositional history of this region.

We have been studying the time-progressive change of diatom flora at Site 997 by quantitatively observing the flora in 141 samples selected from the entire sequence recovered from Holes 997A and 997B. These samples were chosen to represent a time interval of 50 k.y. Some of the results currently obtained through this study are presented in this data report.

METHODS AND PROCEDURES

A set of strewn slides was prepared by a modified technique of the one described in Koizumi (1980, 1992). After drying in an oven at 50°C for 24 hr, 0.1g (\pm 5%) of the sample was boiled in a 100-mL beaker with \sim 10 mL of hydrogen peroxide solution (15% strength) for several minutes, and then 20 mL of 10% hydrochloric acid solution was added. After boiling 5 min, the beaker was filled with distilled water and left to stand for 5 hr. The supernatant of the suspension was poured off, and the beaker was filled again with distilled water. This decanting process was repeated four times to dilute acid from the suspension. The residue was diluted with 100 mL of distilled water and homogenized for about 3 seconds in an ultrasonic bath. By using a micropipette, 0.5 mL of this solution was spread on a square cover glass (18 \times 18 mm) and dried on a hot plate at 50°C. The prepared cover glass was mounted on a glass slide by using Pleurax.

All diatoms were identified and counted under a light microscope with magnification of 600 \times until the total number exceeded 200 (resting spores of *Chaetoceros* spp. were not included). The counting was accomplished by observing up to ten traverses spanning the entire width of cover glass. For slides with low concentrations of diatoms, the total counts did not reach 200 specimens. Specimens representing more than one-half of a valve of centric diatom were counted, except for genus *Rhizosolenia* and *Proboscia* for which caryptae were counted. For the pennate diatoms, one half of the observed number of the end parts were counted as the respective valves. Because the weight of sediment on a cover glass is calculable, the abundance of diatom valves (#/g) was obtained from a number of transects and the

total counts of diatom valves. The result obtained from this counting procedure is presented in Table 1.

DIATOM ABUNDANCE AND SEDIMENTATION RATE

The diatom abundance fluctuates significantly between 0 and several millions per 1 g of sediment (Fig. 2). In the lower sequence (Miocene and lower Pliocene, 750–300 mbsf), the occurrence of diatoms is generally high between 400 and 600 mbsf but is greatly diminished both below and above this interval. In the upper 300-m sequence corresponding to the upper Pliocene and Quaternary, meanwhile, there are four short intervals showing particularly high diatom numbers: 240–270, 150–180, 70–120, and 40–60 mbsf. In the other intervals, the abundance drops to very low levels ($<1 \times 10^6$).

According to the shipboard investigation of smear slides (Shipboard Scientific Party, 1996), calcareous nannofossils occupy 10% of the sediment throughout the entire sequence except in the uppermost 20 m, where they occupy 20% of the sedimentary composition (Fig. 2). Clay minerals, meanwhile, fluctuate greatly between 40% and 80%, and there seems a reversed relationship between the diatom number and clay mineral abundance. Although the shipboard party postulated an increased supply of diatoms as the cause of the increased sedimentation rate, the diatom number is fairly high in some intervals of the upper 110-m sequence where the sedimentation rate is significantly slow.

A comparison in distribution of the averaged diatom abundances within the upper 110-m sequence and in the lower sequence revealed an opposite trend (Fig. 3). The diatom abundance shows a negative trend with the decreased sedimentation rate within the upper sequences, whereas the relationship is positive in the lower sequence. The negative correlation in the upper sequence means that the increase of sedimentary particles other than diatoms had contributed to the increased sedimentation rate. Also, the abundance of clay-size particles decreases drastically in some intervals of the upper sequence, contrasting sharply with the relatively stable trend observed in the lower sequence (Fig. 2). Such a drastic reduction of the clay-sized particles indicates winnowing in the upper sequence.

On the other hand, the weak but definitely positive correlation between the averaged diatom abundance and sedimentation rate means that an increased supply of diatoms had contributed to the increased sedimentation rate for the uppermost Miocene to lowest Pliocene sequence, where the diatom abundance is significantly higher than the adjoining intervals (Fig. 2). This interpretation is also supported by the significant increase in resting spores of genus *Chaetoceros* in this high sedimentation-rate interval (Fig. 4).

STRATIGRAPHIC DISTRIBUTION OF MAJOR SPECIES

Age assignment based on the calcareous nannofossil biostratigraphy (Okada, Chap. 33, this volume) was the basis for the age model used in this study: the oldest sediment recovered from Hole 997B is

¹Paull, C.K., Matsumoto, R., Wallace, P.J., and Dillon, W.P. (Eds.), 2000. *Proc. ODP, Sci. Results*, 164: College Station, TX (Ocean Drilling Program).

²Department of Earth and Planetary Sciences, Graduate School of Science, Hokkaido University, N10 W8, Kita-ku, Sapporo 060-0810, Japan. Correspondence author: ikeda@cosmos.sci.hokudai.ac.jp

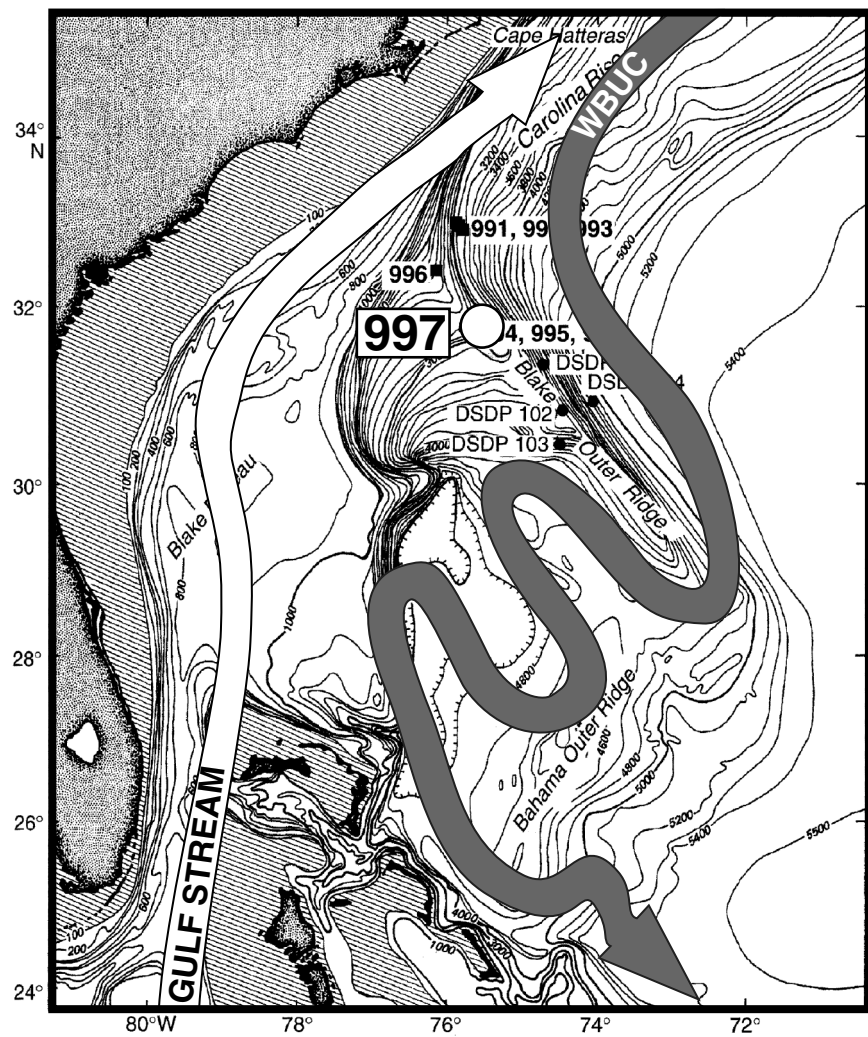


Figure 1. Location of Leg 164 Site 997 and the course of the two major current systems. The course of the Western Boundary Undercurrent (WBUC) and the Gulf Stream is adopted from Faugères et al. (1993).

6.6 Ma. The most abundant species in Holes 997A and 997B is *Paralia sulcata*, a typical shallow-water species, and there are other shallow-water species also occur as major components of the flora (Fig. 4). The cold-water species such as *Actinocyclus curvatus* and *Coscinodiscus marginatus* are present, but their numbers are limited (Table 1). Although the absolute abundance is low, a group of freshwater species such as *Achnanthes* spp., *Aulacoseira* spp., *Cocconeis* spp., and *Opephora* spp. register temporary increases at 3.2, 2.6, 2.4, and 1.1 Ma (Table 1). This evidence indicates a heavy reworking of diatoms. Probably the majority of reworked diatoms were transported from nearby shallow areas and not from the subarctic Atlantic by the WBUC.

Taxa indicating high primary production, such as *Thalassionema nitzschiooides* and resting spores of genus *Chaetoceros*, are abundant in the intervals corresponding to the time periods of 6.0–4.8 and 3.0–2.8 Ma. Because the total diatom abundance is also high within these intervals, it is postulated that the primary production was increased during these time intervals at this site. The increased abundance of reworked brackish water species *P. sulcata* and *Melosira westii* in these intervals may also indicate an increased productivity at a shallow source area. Other major taxa include warm-water species such as *Thalassiosira eccentrica*, *Azpeitia nodulifera*, *Fragilariopsis dolliola*, and *Planktoniella sol*. The distribution characteristics of these major taxa is correlative to the sea-level curve of Haq et al. (1987) in the upper sequence, but the relationship is not clear in the lower sequence. The floral succession of the last six and a half million years is summarized into five stages.

Stage 1: Low-Productivity Stage (6.6–6.0 Ma)

Diatoms are scarce, and the maximum abundance reaches only to 1.1×10^6 /g.

Stage 2: High-productivity Stage (6.0–4.8 Ma)

Diatoms are generally high but fluctuating throughout this interval (on the order of 10^6 – 10^7). In addition to the shallow-water species *P. sulcata* and *M. westii*, *T. nitzschiooides*, a high-productivity indicator, and *T. eccentrica*, a pelagic warm-water species, are abundant. Therefore, it is likely that the productivity was high at this site as well as at nearby continental shelves, possibly because of an eastward shift of gyre margin. This high-productivity period doesn't correlate to the sea-level curve that shows a gradual rise of sea level throughout this period.

Stage 3: Low-productivity Stage (4.8–3.6 Ma)

Diatom abundance is consistently low (in the order of 10^4 – 10^5 /g), and the maximum value recorded in this interval is 1.9×10^6 . The abundance pattern also doesn't show a significant correlation with the sea-level curve.

Stage 4: Fluctuating Productivity Stage (3.6–0.8 Ma)

Diatom abundance fluctuates as in Stage 2, but the wave length is longer and the degree of fluctuation is much greater. There seems to

Table 1. Distribution chart of diatom species at Site 997.

Table 1 (continued).

Core, section, interval (cm)	Depth (mbsf)	Age (Ma)	Abundance (10 ⁶ g)	<i>Delphineis angustata</i> <i>D. surirella</i> <i>D. spp.</i>	<i>Denticulopsis dimorpha</i> <i>D. hastedii</i>	<i>Diploneis</i> spp. <i>Epithemia</i> spp. <i>Fragilariopsis dolitala</i> <i>Glyptothecum acus</i>	<i>Goniothecium</i> spp.	<i>Grammatophora</i> spp. <i>Hantzschia amphioxys</i> <i>Hemiaulus</i> spp. <i>Hemidiscus caniformis</i> <i>H. ovalis</i>	<i>Hyalodiscus</i> sp. A <i>H. amphioxys</i> <i>Koizumiadaoroi</i> <i>K. tatsunokuchiensis</i> <i>Lylella hemmedyi</i>	<i>Melosira architectonitis</i> <i>M. westii</i> <i>M. spp.</i>	<i>Neodaphneis pelagica</i> <i>Neodenitella kamchatkica</i>	<i>N. seminae</i> <i>Nitzschia constricta</i> <i>N. cylindrica</i> <i>N. granulata</i> <i>N. fossilis</i>	<i>N. jovaeae</i> <i>N. lorenziana</i> <i>N. marina</i> <i>N. miocenica</i> <i>N. pandiformis</i> <i>N. reinholdii</i>
164-997A-													
1H-1, 39-41	0.39	0.02	11.50										
1H-CC, 0-1	2.75	0.11	17.57										
2H-2, 114-116	5.54	0.22	5.12										
2H-4, 39-41	7.79	0.29	18.86										
2H-5, 114-116	10.04	0.35	172.87	1		2		2		2			
3H-1, 39-41	12.79	0.43	57.93	1		3		1		2			
3H-2, 114-116	15.04	0.48	3.94										
3H-4, 114-116	18.04	0.53	0.25										
3H-6, 39-41	20.29	0.58	4.36										
4H-1, 114-116	23.04	0.62	311.68	7		4		1		1			
4H-3, 39-41	25.29	0.67	3.99	1				2					
4H-6, 114-116	30.54	0.76	0.00										
5H-2, 39-41	33.29	0.81	538.12			2							
5H-3, 114-116	35.54	0.85	273.74	1		5		1					
5H-5, 39-41	37.79	0.89	455.78	1		6	1	3					
5H-6, 114-116	40.04	0.93	467.42			8	1	2					
6H-2, 39-41	42.79	0.98	341.33			10							
6H-4, 39-41	45.79	1.08	239.26	1	1	6		1					
6H-5, 114-116	48.04	1.26	724.10			7		1					
6H-7, 39-41	50.29	1.32	804.96	1	6	2		1					
8H-2, 114-116	55.54	1.46	0.97										
8H-4, 49-51	57.94	1.50	0.73										
8H-5, 114-116	60.09	1.52	0.00										
9H-1, 114-116	62.54	1.56	0.00										
9H-3, 114-116	65.54	1.60	0.00										
9H-5, 49-51	67.89	1.63	0.00										
9H-6, 114-116	70.04	1.65	0.61										
10H-2, 49-51	72.79	1.69	19.72										
10H-4, 49-51	75.74	1.79	479.14	4		6		2	1				
10H-5, 114-116	77.89	1.86	326.21	10		2		1					
10H-7, 49-51	80.24	1.94	129.82	5		1		1					
11H-1, 114-116	81.54	1.97	524.58	8		8		1					
11H-2, 114-116	83.04	2.00	95.41	6		1		1					
11H-4, 49-51	85.39	2.04	431.02	4		4	1	1					
11H-5, 114-116	87.54	2.08	83.54	4		1							
11H-CC, 29-30	90.39	2.14	35.07	2									
12H-2, 114-116	92.54	2.18	73.66	2		3		1					
12H-4, 114-116	95.54	2.24	121.43	3		4							
12H-6, 49-51	97.81	2.28	9.40	1									
13H-1, 49-51	99.89	2.32	139.68	8		3	1	2					
13H-3, 114-116	102.62	2.37	344.17	10		6		1					
13H-5, 114-116	105.62	2.43	260.93	5	2	1		1					
13H-7, 49-51	107.97	2.48	200.94	9		2	1	1					
14H-2, 114-116	110.37	2.51	251.01	1	5	2		2					
14H-4, 49-51	112.72	2.52	82.20	2		1		1					
14H-6, 114-116	115.72	2.54	388.35	11		4		3	1				
14H-7, 114-116	117.87	2.55	338.18	5		6		2					
15H-2, 49-51	120.39	2.56	316.43	8		7							
15H-3, 114-116	122.54	2.57	323.91	16		1	9	1	2				
15H-5, 114-116	125.54	2.59	34.90										
15H-7, 49-51	127.89	2.61	211.22	2	12	7		1					
16H-2, 49-51	129.89	2.62	37.98	1		1							
16H-4, 49-51	132.89	2.64	18.52	1		2		1					
16H-5, 114-116	135.04	2.65	7.95										
17H-1, 49-51	137.89	2.67	17.42			1							
17H-2, 114-116	140.04	2.68	32.88										
17H-4, 114-116	143.04	2.70	50.08	1	1	4	1	1	1	1			
17H-6, 49-51	145.29	2.72	362.85	1	4	1	2	1	1	20			
19H-1, 49-51	148.39	2.74	335.57	3	2	1	1	1	1	8			
19H-3, 114-116	151.37	2.76	82.42	3	1	1		1	1	7			
20H-2, 49-51	159.39	2.80	370.21	2	6	1	8	1	1	4			
20H-7, 49-51	166.89	2.85	554.55	1	5	2		1	2	11			
22X-2, 31-33	174.41	2.89	629.45	2	3	5		1	1	15			
22X-7, 28-30	181.27	2.92	652.67	4	3	2	1	3	1	4			
26X-1, 38-40	203.78	3.05	8.15							1			
27X-1, 30-32	212.3	3.09	44.23	1				1	1	7			
27X-6, 30-32	219.44	3.13	10.96							1			
28X-CC, 0-1	225.06	3.16	22.70	1		1		1		3			
30X-2, 29-31	234.09	3.21	135.13	1	1	6		1	2	122			
31X-1, 60-62	241.5	3.25	198.01	1	7	4		3	1	1	12		
31X-CC, 0-1	248.59	3.29	618.86	2		6		1	1	14			
32X-5, 27-29	256.77	3.33	12.31	1		1							
34X-3, 27-29	264.3	3.38	14.37	2		1							
35X-2, 29-31	271.24	3.41	493.92	1	9	2		3		15			
36X-2, 30-32	279.85	3.46	44.75	3	3	1		2	1	5			
36X-CC, 30-32	285.53	3.49	188.45	1	3	6		1	1	34			
37X-4, 30-32	293.7	3.54	26.98					1		6			
38X-3, 30-32	301.8	3.58	15.15							1	1		
39X-1, 30-32	308.4	3.62	12.44					1			1		
39X-6, 30-32	315.9	3.67	68.35						1	4	6		

Table 1 (continued).

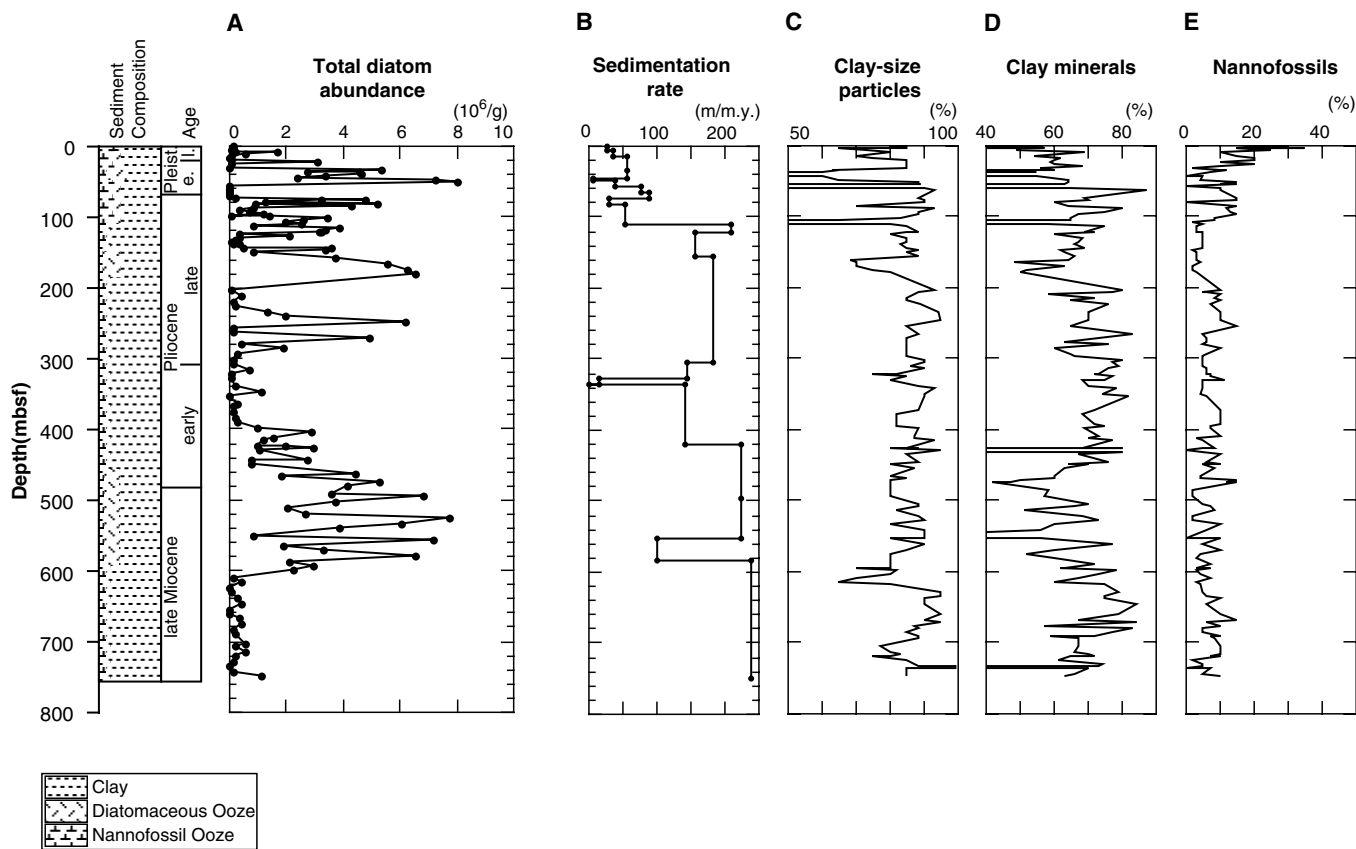


Figure 2. Stratigraphic variations in the total abundance of diatom valves and other related parameters plotted against the sub-bottom depth. The data, except for the diatom abundance, are taken from Shipboard Scientific Party (1996).

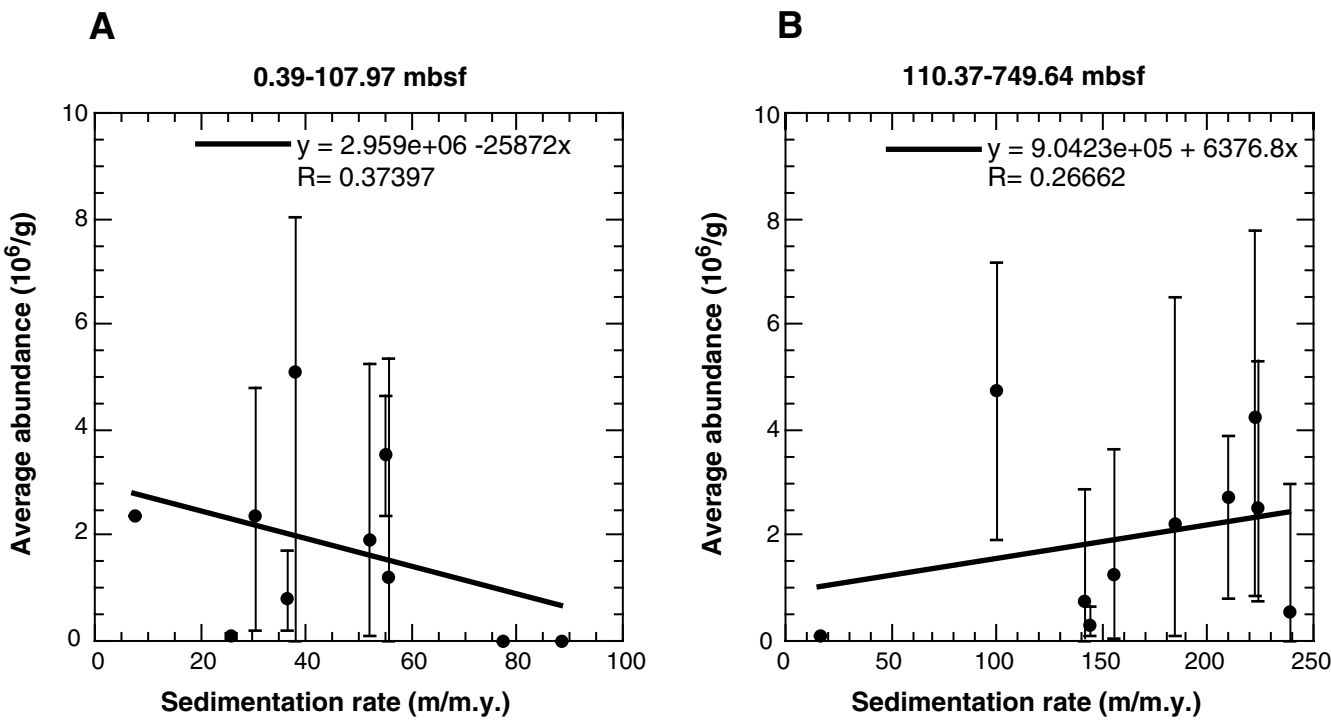


Figure 3. Correlations between the average abundance of diatoms and sedimentation rates in the upper (0–110 mbsf) and lower (110–750 mbsf) sequences.

be some correlation between the diatom abundance and the eustatic curve in the upper part: the higher abundances of 2.1–1.8 Ma and 1.4–0.8 Ma correspond to the highstand phases (Fig. 4). As was discussed above, however, the higher total diatom abundances are result of reduced clay supply but not of increased productivity. Contrary, the higher diatom flux of 3.0–2.8 Ma, which corresponds to regression phase, is a result of the increased supply of diatom valves, possibly because of an increased productivity.

Stage 5. Low-productivity Stage (0.8–0 Ma)

Although there are some short exceptions, the diatom abundance is low. This interval corresponds to the lowstand phase, concordant with the trend observed in the upper part of the underlying stage.

ACKNOWLEDGMENTS

We thank the co-chiefs, shipboard scientists, technicians, and crews of the *JOIDES Resolution* for their assistance and cooperation in obtaining the samples. Our thanks is also extended to Dr. K. Kashima, Kyushu University, for his valuable advice.

REFERENCES

- Cande, S.C., and Kent, D.V., 1995. Revised calibration of the geomagnetic polarity timescale for the Late Cretaceous and Cenozoic. *J. Geophys. Res.*, 100:6093–6095.
- Faugères, J.C., Mézerais, M.L., and Stow, D.A.V., 1993. Contourite drift types and their distribution in the North and South Atlantic Ocean basins. *Sediment. Geol.*, 82:189–203.
- Haq, B.U., Hardenbol, J., and Vail, P.R., 1987. Chronology of fluctuating sea levels since the Triassic. *Science*, 235:1156–1167.
- Koizumi, I., 1980. Neogene diatoms from the Emperor Seamount Chain, Leg 55, Deep Sea Drilling Project. In Jackson, E.D., Koizumi, I., et al., *Init. Repts. DSDP*, 55: Washington, (U.S. Govt. Printing Office), 387–400.
- , 1992. Diatom biostratigraphy of the Japan Sea: Leg 127. In Piscesciotto, K.A., Ingle, J.C., Jr., von Breymann, M.T., Barron, J., et al., *Proc. ODP, Sci. Results*, 127/128 (Pt. 1): College Station, TX (Ocean Drilling Program), 249–289.
- Shipboard Scientific Party, 1996. Site 997. In Paull, C.K., Matsumoto, R., Wallace, P.J., et al., *Proc. ODP, Init. Repts.*, 164: College Station, TX (Ocean Drilling Program), 277–334.

Date of initial receipt: 27 April 1998

Date of acceptance: 13 October 1998

Ms 164SR-231

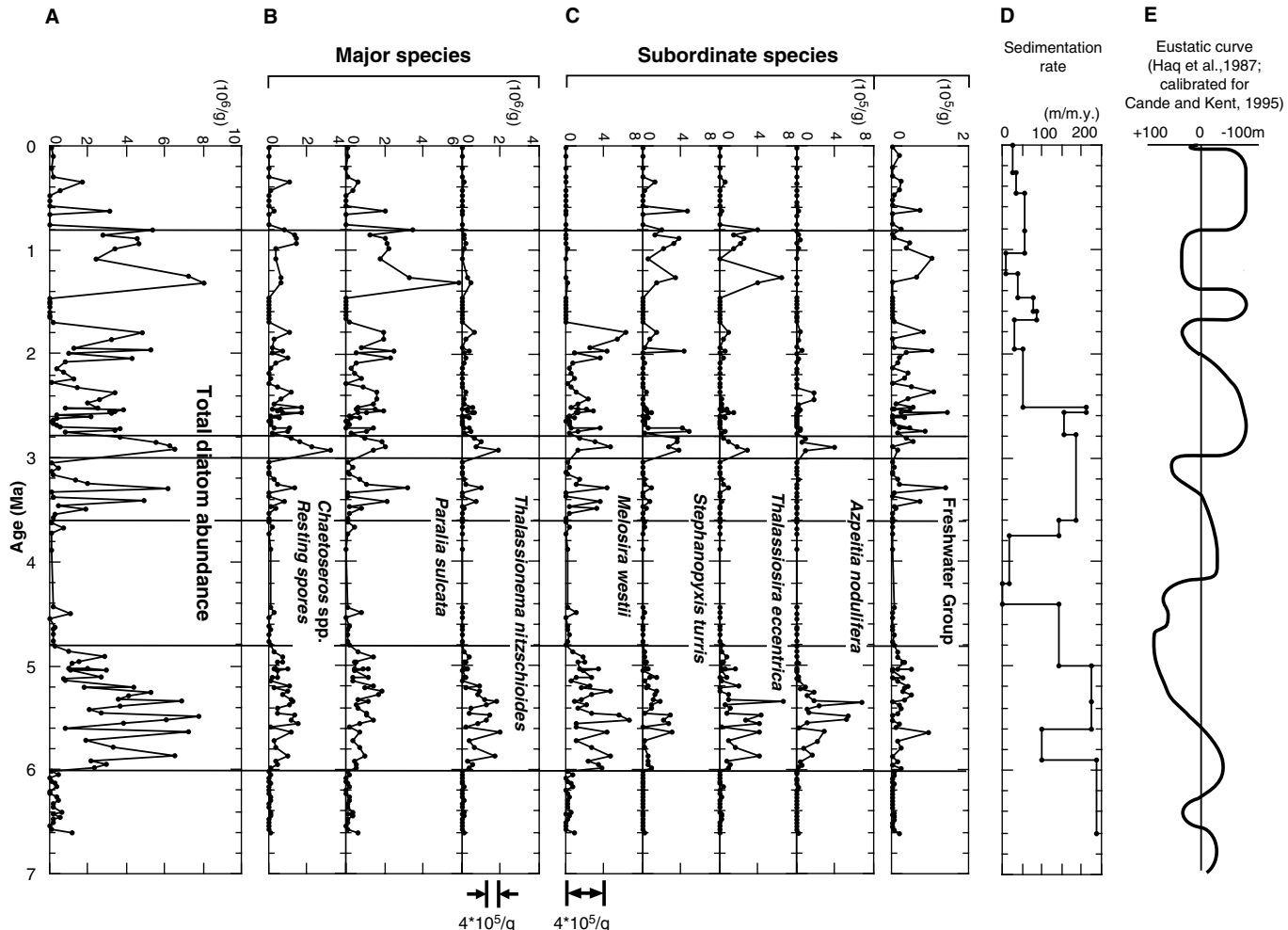


Figure 4. Time series of (A) total abundance of diatom valves, (B) abundances of the major species, (C) abundances of subordinate species, (D) sedimentation rate, and (E) eustatic curve (Haq et al., 1987). Note the difference in the horizontal (abundance) scales of B and C. The age assignments for the eustatic curve are calibrated by Cande and Kent (1995). The eustatic curve of Haq et al. (1987) is modified by the recent paleomagnetic chronology of Cande and Kent (1995).